Available online at www.sciencedirect.com
ScienceDirect
Surface & Coatings Technology 201 (2006) 4460–4466
www.elsevier.com/locate/surfcoat

# Oxidation resistance of magnetron-sputtered CrAlN coatings on 430 steel at 800 °C

A. Kayani [a,*], T.L. Buchanan [a], M. Kopczyk [a], C. Collins [a], J. Lucas [a], K. Lund [a], R. Hutchison [a], P.E. Gannon [a], M.C. Deibert [a], R.J. Smith [a], D.-S. Choi [b], V.I. Gorokhovsky [c]

[a] Montana State University-Bozeman, MT 59717, United States
[b] Kangwon National University, Republic of Korea
[c] Arcomac Surface Engineering, LLC-Bozeman, MT 59715, United States

Available online 8 September 2006

**Abstract**

The requirements of low cost and high-temperature corrosion resistance for bipolar interconnect plates in solid oxide fuel cell stacks have directed attention to the use of metal plates with oxidation resistant coatings. We have investigated the performance of steel plates with homogenous coatings of CrAlN. The coatings were deposited using RF magnetron sputtering, with Ar as a sputtering gas and N gas added during the growth process. The Cr/Al composition ratio in the coatings was varied in a combinatorial approach. The coatings were subsequently annealed in air for up to 25 h at 800 °C. The composition of the coated plates and the rate of oxidation were characterized using Rutherford backscattering (RBS) and non-Rutherford backscattering analysis. From our results, we conclude that Al rich coatings are more susceptible to oxidation than Cr rich coatings and Cr/Al ratio of 0.9 offers the best resistant to oxidation.


*Keywords:* CrAlN; SOFC interconnect; Coatings; Ion beam analysis; Corrosion resistance

## 1. Introduction

Solid oxide fuel cells (SOFC) are becoming increasingly attractive as a way of converting chemical energy into electrical energy by means of the electrochemical combination of hydrogen and oxygen via an ion-conducting solid oxide electrolyte. The operational requirements of high ionic conductivity and good catalytic performance in the fuel cell must be balanced against the practical requirements of low cost and high-temperature corrosion resistance for components in the fuel cell stack [1]. Of particular interest in our work is the bipolar plate serving as the current collector or interconnect between adjacent cells of the SOFC stack. The interconnect must not only retain low electrical resistivity throughout the operating lifetime of the fuel cell, but must also have good surface stability, necessitating that thermal expansion and other physical properties be compatible with the materials in the stack [2]. Doped $LaCrO_3$ plates have worked well for cells operating at 1000 °C, but suffer from high cost as well as difficulties in fabrication. The recent trend towards lower operating temperatures (500–750 °C) may enable the use of more cost-effective materials. A thorough evaluation of several heat-resistant alloys with a variety of compositions led to the conclusion that it would be difficult for most traditional alloys to meet the material requirements of long-term operation above 700 °C [3]. Alloys of bcc, ferritic stainless steels appear to have thermal expansion coefficients that are well matched to other components in the stack, but do not possess the high electrical conductivity needed for required operation. The authors conclude that for improved oxidation resistance and electrical conductivity, either new alloys need to be developed, or surface engineering of existing alloys is required [3]. Among candidate materials in the former category is Crofer22 APU, an Fe–Cr based ferritic stainless steel with additional manganese (available from ThyssenKrupp VDM). The present work falls into the latter category of surface engineering, namely, the use of coatings to improve oxidation resistance while maintaining acceptably low resistivity values. Related research on surface engineering includes the use of conducting oxide coatings and thermal nitriding [4]. The use of coatings for this application brings with it

* Corresponding author.
*E-mail address:* kayani@physics.montana.edu (A. Kayani).

0257-8972/$ - see front matter © 2006 Elsevier B.V. All rights reserved.
doi:10.1016/j.surfcoat.2006.08.049

an additional set of problems, namely, guaranteeing the integrity of the coating with respect to adhesion, wear resistance, and detrimental effects associated with interdiffusion between coating and substrate material. On the other hand, using coatings enables the use of inexpensive alloys that would otherwise be ruled out because of their poor oxidation resistance.

The use of coatings to improve oxidation resistance on metal alloys has been known for many years. We selected the Cr–Al–N system for this study because it not only offers oxidation resistance at temperatures up to 900 °C [5,6], but also provides a high wear resistance that is typical of many metal nitrides [7]. For our previous study, we used multilayer and nanolayer structures, consisting of AlN and CrN, to study the affect of a layered structure and individual layer thickness on the oxidation kinetics for the coating [8,9]. In our present work we use homogeneous CrAlN coatings, deposited by magnetron sputtering, to study the affect of the Cr/Al ratio on oxidation kinetics.

Chromium nitride is a good oxidation resistant material with anti-corrosive properties. Its uses include applications in metal forming and plastic molding [10,11]. It is presently known that exposing CrN to oxygen at elevated temperatures leads eventually to loss of nitrogen and the formation of $Cr_2O_3$ [12] (which is a semiconductor with a sufficiently low resistivity for use in interconnect applications at an operating temperature of 800 °C [13]). The oxidation of AlN leads to the formation of $Al_2O_3$ (alumina) which has an unacceptably low conductivity for use as an interconnect material, yet alumina is known to be a good oxidation-resistant barrier. In our study, using an RF and DC magnetron sputtering technique, we deposited coatings of varying Cr/Al ratios onto a 430 stainless-steel plate sample substrate, the details of which will be addressed later.

Deposition of coatings using magnetron sputtering has many advantages. It is a low pressure sputtering process offering a great deal of control of the deposited ion flux species. At sputter deposition pressures below 0.13 Pa we have a collisionless process, and fast neutral particles start to play an important role in film growth. Magnetron action occurs when the magnetic field and electric fields are normal to each other. Therefore the majority of ionization occurs in the center of an electron cloud. The ions formed are instantly attracted to the negatively biased target where they collide with its surface, causing surface atoms from the target material to be ejected (sputtered). Under the influence of the electric field present, electrons are not allowed to move freely, so very few of them strike the substrate. The target on the other hand comes under fierce ion bombardment, particularly where most of the ions are produced. This action causes localized heating of the target material, which requires cooling.

There are two types of magnetrons, balanced and unbalanced. In a balanced magnetron, the magnetic field of both the core and outer magnets are balanced with each other resulting in nearly all field lines in the magnetic trap to form closed loops between the poles of the magnet. In the cathode area, there is created a wide region containing a strong magnetic field with field lines almost parallel to the target surface. In contrast, the unbalanced magnetron has an imbalance between the magnetic fields of the outer and core magnets. For this particular study balanced magnetron heads were used to deposit CrAlN coatings. For analysis of sample elemental composition and oxidation resistance, Rutherford backscattering spectroscopy (RBS) and non-Rutherford scattering were used. The films were annealed at 800 °C in air for up to 25 h, and subsequently analyzed.

## 2. Experimental procedure

For this initial study, we used a 430 steel plate as the substrate, of dimensions 15.2 × 10.6 cm. An already polished stainless-steel plate was purchased from a local hardware store. This material is sold for use as a heat shield and its finishing process is termed "bright-annealed". Sample coupons of dimension 1 × 2 cm were laser cut from the steel plate in such a way that these coupons were left attached to the plate with a small tab. Sputter coating was carried out at the Montana Microfabrication Facility at Montana State University. This chamber provided by Angstrom Engineering is fitted with three water-cooled balanced magnetron sputter heads mounted 120° apart on the horizontal plane and at an angle of 30° from the normal from the copper sample holder. Each head has a shutter attached for soaking purposes. The sample holder is a circular disk 15.3 cm in diameter which can be rotated. The sample holder is inserted into the sputtering chamber through a load lock. The substrate to sputter-target distance was 18 cm. Ultra high vacuum is created inside the sputtering chamber by a cryogenic pump. Gases used in reactive deposition and for sputtering purposes are introduced into the chamber by separate precision mass flow controllers.

Chromium and aluminum metal targets were used to deposit coatings onto our stainless-steel sample plate at room temperature. The chromium target used an RF power source set at 125 W. For the aluminum target, we chose a DC power source set to 216 W. DC power was chosen for the aluminum target because the sputtering rate of aluminum is low compared to that for chromium. 10 sccm of argon sputtering gas and 10 sccm nitrogen reactive gas were introduced into the chamber via separate mass flow controllers. Gas lines were evacuated for 24 h prior to sputter deposition to minimize the contamination in the gas lines. The sputtering chamber was cryogenically pumped for 24 h, achieving a base pressure in the range of $1.3 \times 10^{-6}$ Pa. The working pressure after introduction of the Ar and N gases, was 0.68 Pa. Both sources were soaked for 15 min before beginning deposition. Deposition time was 4 h. A different Cr/Al ratio in the coating on the sample coupons was obtained depending upon their respective placement in the rectangular sample plate with respect to the Cr and Al gun positions as shown in Fig. 1.

| | | | | |
|---|---|---|---|---|
| A2 | A1 | AC1 | C1 | C2 |
| A4 | A3 | AC2 | C3 | C4 |
| A6 | A5 | AC3 | C5 | C6 |
| A8 | A7 | AC4 | C7 | C8 |
| A10 | A9 | AC5 | C9 | C10 |

Fig. 1. Sample positions on the stainless steel substrate rectangular plate.

Oxidation of the sample coupons was carried out using a temperature controlled standard box furnace operated in air, with no additional features to control humidity or air flow rate. Samples were placed horizontally on a ceramic holder with the coated face upwards at the center of the furnace. The oven temperature was controlled electronically and was ramped to 800 °C at the rate of 3 °C/min. Soak times were incremented to give total oxidation periods of 1, 4, 9, 16, and 25 h. After each increment of oxidation time, the oven was cooled to ambient temperature over a period of 30 min. The samples were removed and placed in a vacuum chamber for ion beam analysis. Measurements are still in progress to determine the Area Specific Resistance (ASR) in ohm-$cm^2$, using standard 4-point probe procedures with Pt paste electrodes on pre-oxidized samples for extended periods of time.

## 3. Results and discussion

Fig. 1 shows the coupon sample positions on the rectangular steel plate. For this initial study, five coupons were analyzed, one from each corner plus the one in the center of the plate. These samples were labeled A2, A10, C2, C10 and AC3. The goal was to determine which of these samples demonstrates the best oxidation resistance plus retains enough nitrogen after 25 h of heating and acts as a diffusion barrier for the heavier elements moving from the substrate into the bulk of the coating. The subsequent step would be to choose and analyze other samples from the plate which lie close to the better of the first five.

Ion beam analysis of these samples was performed using a 2 MV single-ended Van de Graaff accelerator at the Ion beams lab facilities at Montana State University (MSU) in Bozeman, MT. Rutherford backscattering spectra (RBS) were recorded using 1.5 MeV beams of $He^+$ and $H^+$ ions, incident normal to the sample surface. Backscattered ions were collected using a silicon surface barrier detector at a scattering angle of 165°, with an exit angle of 15° as measured with respect to the sample's surface normal. RBS spectra were collected for the as-deposited samples before heating as well as after successive oxidation periods of heating at 800 °C for heating times totaling 1, 4, 9, 16 and 25 h. Since the samples were removed from the oven after each oxidation period for ion beam analysis, they were thereby subjected to some thermal cycling, which may have affected the coatings. Composition profiles for the as-deposited samples (before oxidation) were generated using SIMNRA computer simulations of the spectra as the basis for elemental composition percentages [14]. The elemental concentrations for samples A2, A10, C2, C10 and AC3 are listed in Table 1. Rutherford backscattering is particularly useful for obtaining concentration depth profiles for the heavier elements in the coating. However it is somewhat limited in detecting light elements such as O and N due to the quadratic dependence of the Rutherford cross section on the atomic number of the target atom. Therefore, a 1.5 MeV $H^+$ beam was used to take advantage of the non-Rutherford enhancement in the cross section of O and N at this energy. The set of target composition profile parameters in the SIMNRA program was adjusted until a single set of parameters accurately simulated both the $He^+$ and $H^+$ RBS spectra. In some cases there is a rapid decrease in N content following the initial one-hour heat treatment. We attribute this decrease to several mechanisms: transformation of CrN to $Cr_2N$ [13,15], transformation of AlN to $Al_2O_3$, and loss of N to the vacuum. We attribute the gradual loss of N during subsequent annealing to the transformation of $Cr_2N$ to $Cr_2O_3$. The total as-deposited N content varies from sample to sample due to the varied Cr/Al ratios obtained during the coating process. The variation in the nitrogen content is relatively small and can be taken as constant (see Table 1) for all of the samples, and therefore we will consider the Cr/Al ratio as the important parameter for the oxidation properties of each sample.

Table 1
Survey of as deposited coating compositions

| Sample | Cr % | Al % | N % | Thickness (nm) | Thickness ($10^{15}$ atoms/$cm^2$) |
|---|---|---|---|---|---|
| A2 | 4.5 | 38 | 57.5 | 722 | 8500 |
| AC3 | 15 | 28 | 57 | 552 | 6500 |
| A10 | 10.5 | 30 | 59.5 | 382 | 4500 |
| C2 | 19 | 21 | 60 | 552 | 6500 |
| C10 | 31 | 11 | 58 | 493 | 5800 |

A depth scale of $10^{15}$ atoms/$cm^2$ is characteristic of RBS analysis which describes the number of target atoms visible to the incident ion beam. If sample densities are known, this parameter is readily convertible to a linear depth scale. Since we had no prior knowledge of the densities of the as-deposited coatings, the average atomic density of cubic CrN and hexagonal AlN ($1.2\times10^{23}$ atoms/$cm^3$) was used to establish that $1000\times10^{15}$ atoms/$cm^3$ corresponds to a depth of 85 nm. Based upon this quantity, the thickness of each coating was calculated and is listed in Table 1.

The thickness and Cr/Al ratios of the coating for each sample varied due to their respective positions relative to the Cr and Al sputtering guns. The coatings in the five samples analyzed, demonstrate greatly varying characteristics when subjected to the same high-temperature oxidizing periods. In the as-deposited (non-heated) coating, oxygen is not present and each contains nitrogen as expected from the environment of the sputtering chamber present during the growth process. One of the desirable characteristics we wished to find is that some nitrogen is retained by the coating after the oxidation process, which indicates improved oxidation resistance. The final thickness of these coatings increases with the oxidation process because of the transformation of AlN to $Al_2O_3$ and CrN to $Cr_2O_3$. We expect the dominant phases in the as deposited coatings to be AlN, CrN, and $Cr_{1-x}Al_xN$, as reported in the literature [16].

We first address the results for sample AC3 shown in the left column of Fig. 2. During the heating process at 800 °C, nitrogen is gradually replaced by oxygen. However, after 25 h of oxidation, nitrogen is still present in the coating. In the near surface region, however nitrogen was completely replaced by oxygen. Furthermore, oxygen diffused through the coating, reaching the coating–substrate interface. We also observe that after only 25 h of heating, Fe begins to diffuse into the coating. The diffusion depth of Fe from the substrate interface into the coating is about 80–90 nm. We expect further Fe diffusion into the coating if the sample is subjected to subsequent extended periods of heating.

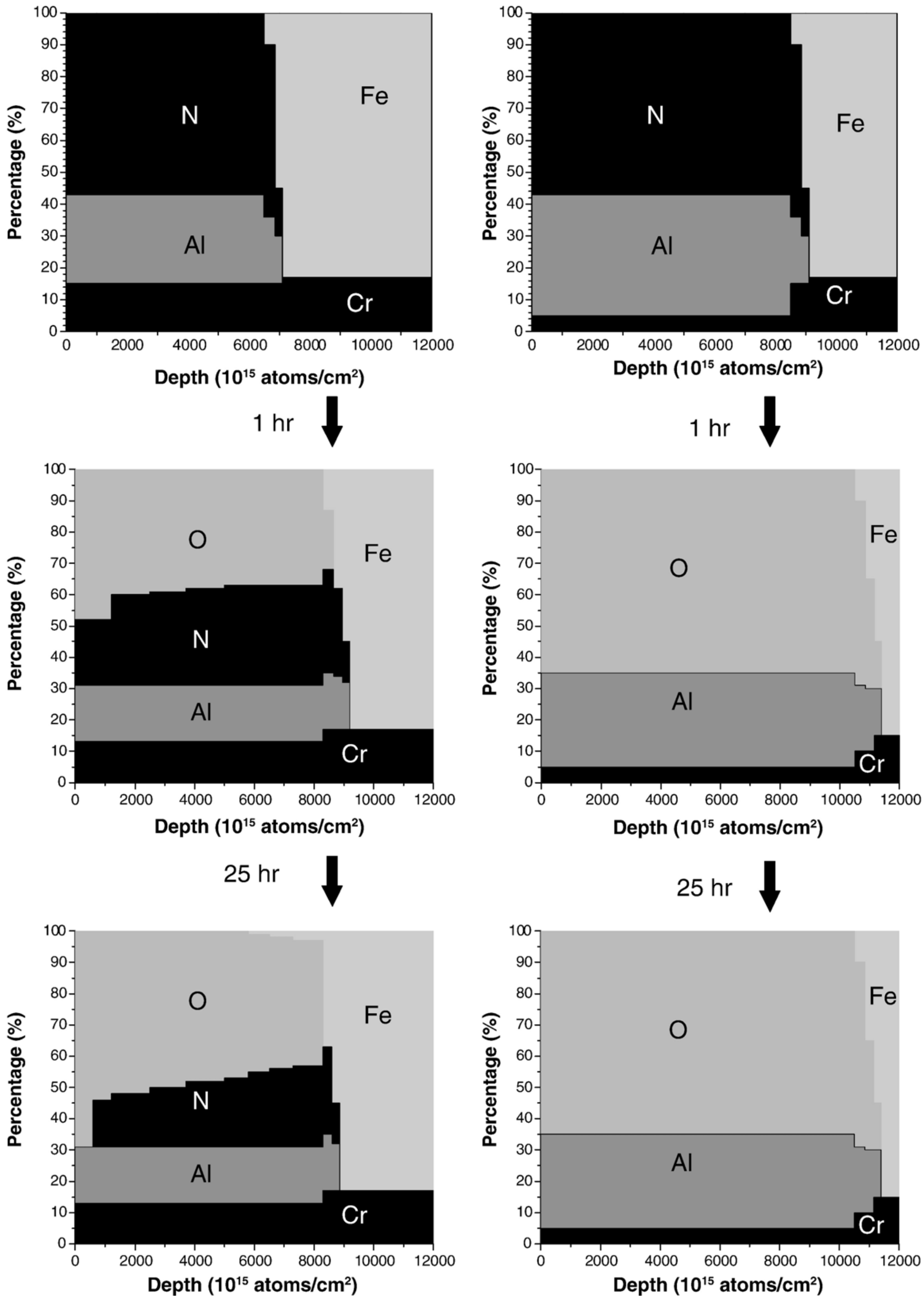


Fig. 2. Composition profile evolution with annealing time for the samples AC3 (left column) and A2 (right column).

In the coating of sample A2, nitrogen is completely replaced by oxygen after only 1 h of heating at 800 °C, as can be seen in Fig. 2, right column. No diffusion of Fe or any heavy elements from the substrate into the coating was observed after the 25-hour period of annealing. The coating of sample A2 is Al rich at 38% Al content. The most probable oxides formed in the coating are $Al_2O_3$ and $Cr_2O_3$. The performance of the coating A2 is not as good as that for sample AC3. The primary difference between the coatings is their respective Cr/Al ratio content. The coating AC3 has a greater Cr content than the coating A2 and appears to have oxidized far less.

During the heating process at 800 °C, for the coatings C2 and C10, nitrogen is gradually replaced by oxygen, and after 25 h of oxidation, nitrogen is still present in the coatings. In the near surface region, as depicted in Fig. 3, nitrogen was completely replaced by oxygen. For sample C10 after 25 h of heating, oxygen was found to have diffused through the coating, reaching the coating–substrate interface. However, for sample C2, the uptake

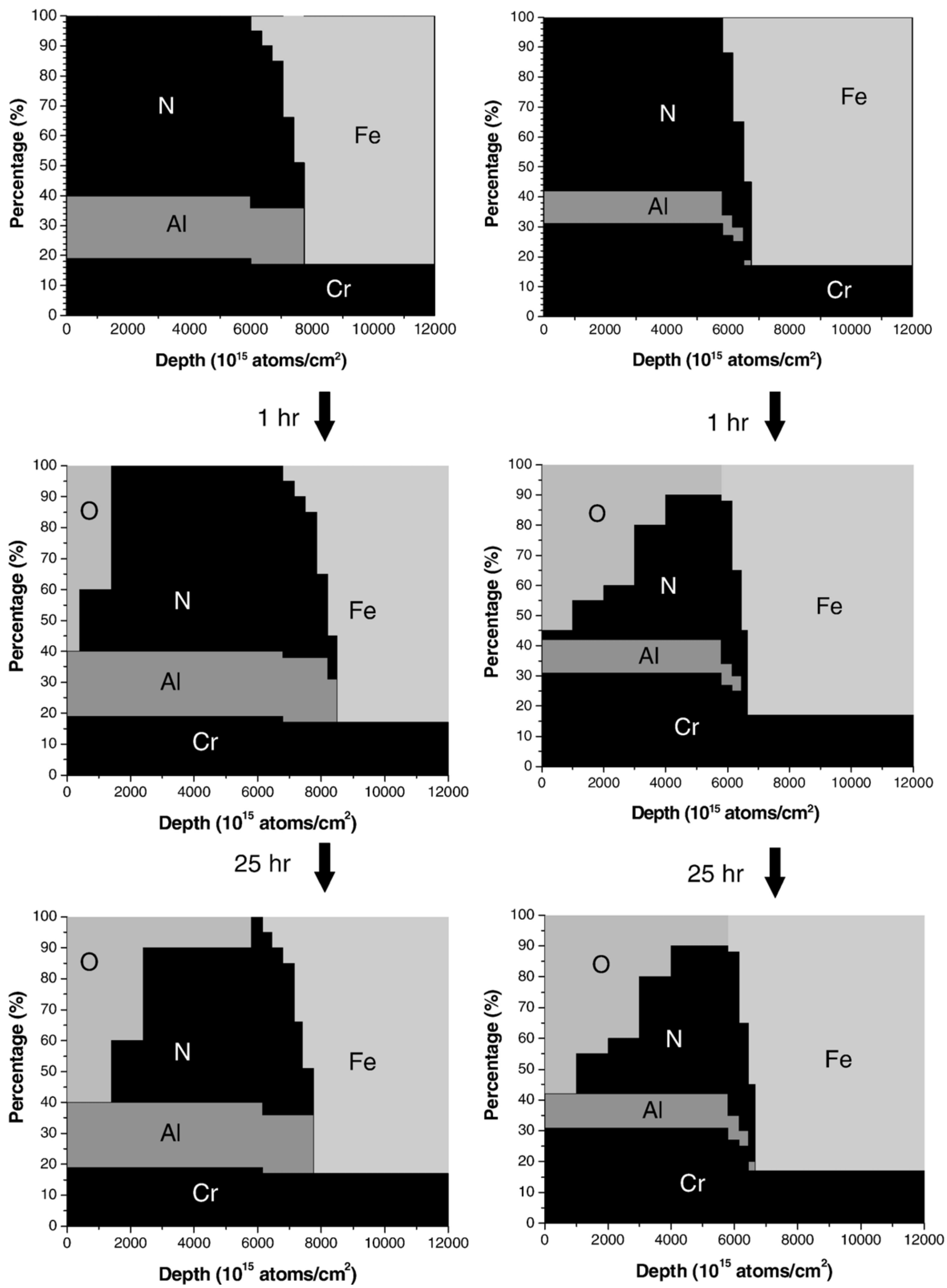


Fig. 3. Composition profile evolution with annealing time for the samples C2 (left column) and C10 (right column).

of oxygen was less than as compared to that for sample C10. No diffusion of Fe into the coating of either sample was observed. The oxidation performance for C2 appears to be as good as that for C10. The primary difference between the coatings of these two samples is that the coating for sample C10 has a higher Cr content than that of C2, but C2 appears to have oxidized less that C10.

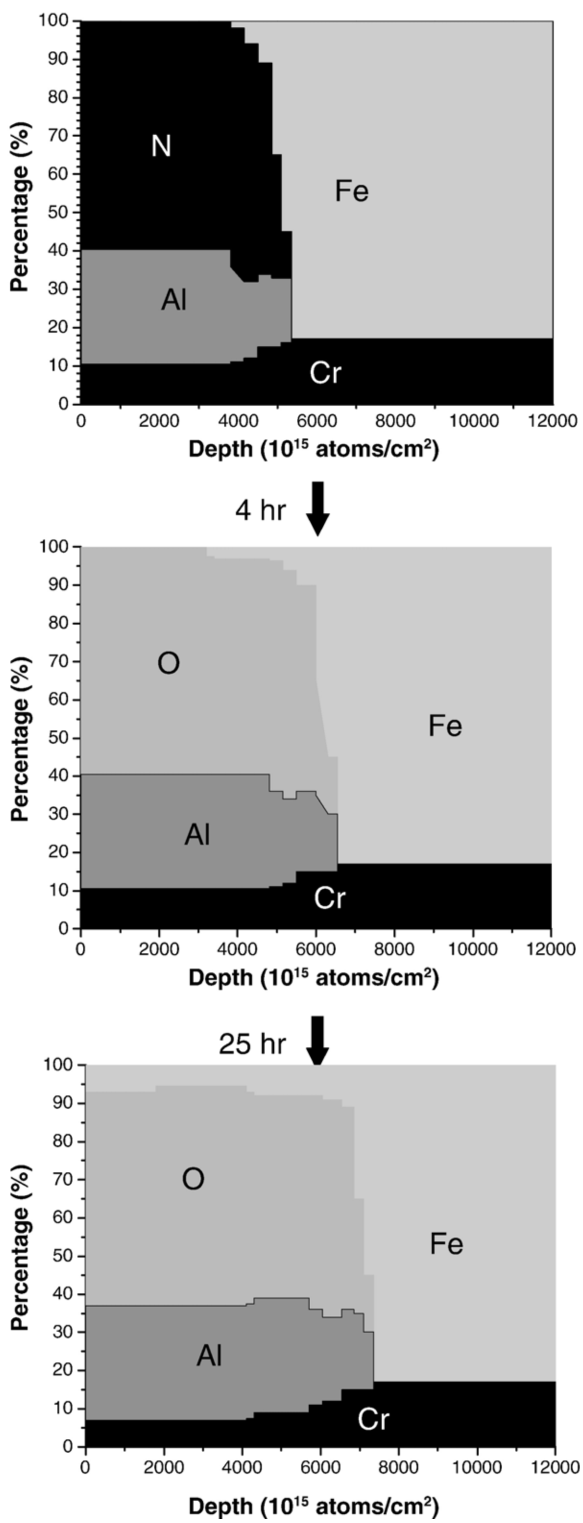


Fig. 4. Composition profile evolution with annealing time for the sample A10.

For the coating of sample A10, nitrogen is completely replaced by oxygen after only an hour of heating. Furthermore, after only this 1 h of heating, oxygen has diffused through the coating, reaching the coating–substrate interface. After 4 h of heating Fe has started diffusing from the substrate up through the coating and after 25 h of heating, Fe has diffused from the substrate, completely through the coating to the surface as seen in Fig. 4. The coating for sample A10 is Al rich. The final thickness of the oxide after 25 h of heating is somewhat greater than what it was when as-deposited, which may be a result of out-diffusion of Fe. Moreover, diffusion of Fe can be enhanced at higher temperatures when the mismatch in the thermal expansion coefficient of the substrate and the coating is more apparent, resulting in film stress and loss of adhesion of the coating at the coating–substrate interface.

In general, the results from ion beam analysis are quantitative and do not depend on the oxide stoichiometry which might change with depth. The results presented here can be contrasted with those reported by Banakh et al. [6] who also studied high-temperature oxidation resistance for sputtered $Cr_{1-x}Al_xN$ films. They report poor oxidation resistance when the concentration $x$ for Al is less than 0.2. Further, for films with $x=0.63$, they report the films being stable up to 900 °C. However, RBS measurements revealed an initial bulk oxygen concentration of approximately 14% in their films, and the annealing time at 900 °C was apparently only 15 min. The sputtered films in our case show negligible oxygen following deposition, and have been annealed for much longer times, but at a slightly lower temperature of 800 °C. From our results, we conclude that coatings with Cr/Al$<$0.5 are more susceptible to oxidation.

## 4. Conclusions

We have shown a quantitative means of comparing the oxidation resistance of coated samples. We report early results for the high-temperature oxidation resistance of 430 stainless steel alloy with a coating of different Cr/Al ratios. The best oxidation resistance was observed for sample C2 with a Cr/Al ratio of 0.9. In subsequent studies, we intend to analyze the sample coupons in the locations near that of sample coupon C2. Future measurements will extend the annealing time to better simulate the interconnect application in a solid oxide fuel cell. Measurements of area-specific resistance at temperatures up to 800 °C for these coated steel disks are still in progress.

## Acknowledgments

We acknowledge the technical assistance of Norm Williams and John Getty at Montana State University. We extend our appreciation to the team at the Montana Microfabrication Facility at Montana State University for their assistance and use of their magnetron sputtering facilities. Work at MSU was supported through MSU-HiTEC funded by the Department of Energy (DOE) under Award No. DE-AC06-76RL01830. However, any opinions, findings, conclusions, or recommendations expressed herein are those of the author(s) and do not necessarily reflect the views of the DOE.

## References

[1] B.C.H. Steele, A. Heinzel, Nature 414 (2001) 345.
[2] Z.G. Yang, J.W. Stevenson, P. Singh, Adv. Mater. Process. 161 (6) (2003) 34.
[3] Z.G. Yang, K.S. Weil, D.M. Paxton, J.W. Stevenson, J. Electrochem. Soc. 150 (9) (2003) A1188.
[4] Z.G. Yang, G. Xia, J.W. Stevenson, Electrochem. Solid-State Lett. 8 (3) (2005) A168.
[5] M. Kawate, A.K. Hashimoto, T. Suzuki, Surf. Coat. Technol. 165 (2003) 163.
[6] O. Banakh, P.E. Schmid, R. Sanjines, F. Levy, Surf. Coat. Technol. 163–164 (2003) 57.
[7] S. PalDey, S.C. Deevi, Mater. Sci. Eng., A. Struct. Mater.: Prop. Microstruct. Process. 342 (2003) 58.
[8] R.J. Smith, C. Tripp, A. Knospe, C.V. Ramana, A. Kayani, Vladimir Gorokhovsky, V. Shutthanandan, D.S. Gelles, J. Mater. Eng Perform. 13 (2003) 295.
[9] A. Kayani, R.J. Smith, S. Teintze, M. Kopczyk, P.E. Gannon, M.C. Deibert, V.I. Gorokhovsky, V. Shutthanandan, submitted for publication to be published Surface and Coatings Technology.
[10] T. Bjfrk, M. Berger, R. Westergard, S. Hogmark, J. Bergstrfm, Surf. Coat. Technol. 22–41 (2001) 146.
[11] O. Knotek, M. Atzor, A. Barimani, F. Jungblut, Surf. Coat. Technol. 21–28 (1989) 42.
[12] F.-H. Lu, H.-Y. Chen, C.-H. Hung, J. Vac. Sci. Technol., A 21 (3) (2003) 671.
[13] K. Huang, P.Y. Hou, J.B. Goodenough, Mater. Res. Bull. 36 (2001) 81.
[14] M. Mayer, SIMNRA User's Guide, Technical Report IPP 9/113, Max-Planck-Institut fur Plasmaphysik, Garching, Germany, 1997.
[15] H.-Y. Chen, F.-H. Lu, J. Vac. Sci. Technol., A 21 (3) (2003) 695.
[16] A.E. Reiter, V.H. Derflinger, B. Hanselmann, T. Bachmann, B. Sartory, Surf. Coat. Technol. 2114–2122 (2005) 200;
M. Kawate, A.K. Hashimoto, T. Suzuki, Surf. Coat. Technol. 165 (2005) 163.